ELSEVIER

www.elsevier.nl/locate/jorganchem

Journal of Organometallic Chemistry 582 (1999) 153–159

Journal of Organometallic Chemistry

Electronic coupling of two $[Cp^*ClM]^+/[Cp^*M]$ reaction centers via π conjugated bridging ligands: similarities and differences between rhodium and iridium analogues☆

Wolfgang Kaim [a,*], Sascha Berger [a], Stefan Greulich [a], Ralf Reinhardt [a], Jan Fiedler [b]

[a] *Institut für Anorganische Chemie der Universität, Pfaffenwaldring 55, D-70550 Stuttgart, Germany*

[b] *J. Heyrovsky Institute of Physical Chemistry, Academy of Sciences of the Czech Republic, Dolejškova 3, CZ-18223 Prague, Czech Republic*

Received 17 July 1998

Abstract

The dinuclear complexes $[Cp^*ClM(\mu\text{-}L)MClCp^*](PF_6)_2$, M = Rh or Ir, L = 3,6-bis(2-pyridyl)-1,2,4,5-tetrazine (bptz) or 2,5-bis(phenyliminoethyl)pyrazine (bpip), are reduced in several chemically reversible steps by up to six electrons to the species $[Cp^*M(\mu\text{-}L)MCp^*]^{n-}$. UV–vis/NIR spectroelectrochemistry and EPR of the paramagnetic states were used to identify the various intermediates. The complexes clearly show a reversible, ligand-centered one-electron reduction (E) preceding the first chloride-dissociative metal reduction step (EC). Metal–metal interaction via the bridging π acceptor ligand L causes a splitting of 310–710 mV between the potentials for the two Cl^--dissociative steps. The second chloride release occurs in EC + E fashion for L = bpip but in a two-electron process for L = bptz. The $M^{II}M^{I}$ mixed-valent species $[Cp^*M(\mu\text{-}L)MCp^*]^+$ could be identified via long-wavelength bands from intervalence charge transfer (IVCT) transitions. All complexes containing at least one chloride-free Cp*M group display intense long-wavelength absorption bands. The iridium complexes are distinguished by more negative potentials of the [Cp*Ir]-containing forms, by slower formation of the $M_2^{I,II}$ mixed-valent intermediate, by larger *g* anisotropy of the paramagnetic forms, and by triplet absorption features in the UV–vis electronic spectra. © 1999 Elsevier Science S.A. All rights reserved.

Keywords: Electrochemistry; EPR; Iridium; Rhodium; Spectroelectrochemistry

1. Introduction

The electronic coupling of one-electron redox processes occurring at individual metal centers as mediated by bridging ions or molecules has played an enormous role in the understanding of intra- and intermolecular electron transfer [1]. Typical examples for compounds with equivalent one-electron redox sites are the ligand-bridged dinuclear ammineruthenium(III,II) complexes where the K_c value varies from less than 10^1 to 10^{15} [2,3].

$$K_c = 10^{\Delta E/59\ mV} = [M^{(n-1)}]^2/[M^n][M^{(n-2)}]$$

$$M^n + M^{(n-2)} \rightleftharpoons 2M^{(n-1)}$$

The latter value was observed for a compound involving the 3,6-bis(2-pyridyl)-1,2,4,5-tetrazine (bptz) as conjugated bridging ligand with low lying π acceptor orbitals and large π^* MO coefficients at the coordinating tetrazine nitrogen centers [3,4].

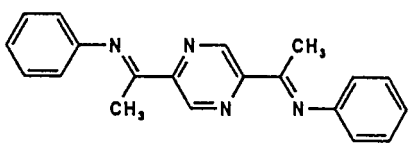

bpip

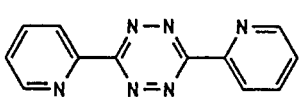

bptz

☆ Dedicated to Professor Peter Jutzi on the occasion of his 60th birthday.

* Corresponding author. Tel.: +49-711-6854170; fax: +49-711-6854165.

E-mail address: kaim@anorg55.chemie.uni-stuttgart.de (W. Kaim)

PII: S0022-328X(98)01027-4

For chemical reactions proper, however, the electronic coupling of processes including a chemical step would be more interesting. Among the most common and well understood of such composite processes are the cyclical EC, EEC or ECE mechanisms where a chemical reaction (C) following electron transfer (E) produces a new species with different electrode potentials which eventually reverts in a second chemical step to the starting compound [5].

We are now reporting an investigation of such an electronic coupling of reaction centers (instead of mere electron transfer centers) which involves two equivalent pentamethylcyclopentadienyliridium centers starting from complex ions $[Cp^*ClIr(\mu\text{-}L)IrClCp^*]^{2+}$, L = 3,6-bis(2-pyridyl)-1,2,4,5-tetrazine or 2,5-bis(phenyliminoethyl)pyrazine (bpip), $Cp^* = \eta^5\text{-}C_5Me_5$. Whereas the bptz bridging ligand is distinguished by its capability to effect strong metal–metal coupling and stabilized paramagnetic species [3,4,6], bpip is a bis(α-diimine) ligand which acts through two different chelate donors, one imine and one azine nitrogen atom per metal center [7,8]. Thus, bpip may be viewed as a centrosymmetrically replicated 2-pyridinecarbaldimine (pyca) system [9,10].

A study of corresponding dirhodium analogues has been described recently [8] and those results will be used here for comparison. When bound to an α-diimine ligand such as 2,2′-bipyridine single Cp^*ClM^+ fragments undergo an ECE process whereby the initial electron acquisition is followed by a rapid dissociation of chloride as the chemical step [11]. The resulting, catalytically active and deeply colored neutral Rh(I) or Ir(I) compounds are reoxidized at a significantly less negative potential upon which they pick up the additional ligand [12–14]. This last step is rather slow as obvious from cyclic voltammetry; the introduction of bulky substituents can considerably delay this process [15,16] and allow for the isolation and structural characterization of the species involved [16].

Compounds of the general type $[Cp^*ClM(\alpha\text{-diimine})]^+$, M = Rh or Ir, have been used for purposes of catalytic hydride transfer, e.g. to protons [11,14,17] or NAD^+ [18]; expectedly, the Rh analogues showed the higher activity.

2. Results and discussion

Complexes $[Cp^*ClIr(\mu\text{-}L)IrClCp^*](PF_6)_2$ were obtained from the ligands L [4,7] and $[Cp^*ClIr(\mu\text{-}Cl)]_2$ [19]. The appearance of close lying pairs of NMR resonance signals for the bpip compounds and for the rhodium complex of bptz suggest the formation of *cis* and *trans* isomers with regard to the positions of Cp* and Cl relative to the π plane of L [8,20]. As has been shown before [8,20], this isomerism has only marginal effects on electrochemistry (Table 1) and absorption spectra (Table 2); compound $[Cp^*ClIr(\mu\text{-bptz})IrClCp^*](PF_6)_2$ was obtained as only one isomer, presumably the *trans* form [20].

In contrast to the Rh^{III} analogues [8], the Ir^{III} precursor compounds are distinguished by weak long-wavelength bands (Table 2), which are assigned to singlet–triplet transitions from the chloride or cyclopentadienide ligands to the metal [12,13,16]. These transitions become detectable because of the high spin-orbit coupling constant of the $5d^6$ center Ir^{III}.

The low-lying π^* acceptor orbitals and the capacity of the ligands for electronic coupling of metal centers leads to a complex picture of the redox processes as followed by cyclic voltammetry (Fig. 1, Table 1), UV–vis/NIR spectroelectrochemistry (Figs. 2 and 3, Table 2) and EPR (for paramagnetic intermediates, Figs. 4 and 5, Table 3). All measurements were done in acetonitrile except for the absorption spectroelectrochemistry of $[Cp^*ClIr(\mu\text{-bpip})IrClCp^*](PF_6)_2$, which was performed in DMF where the reduced forms of the complex were more stable.

The dinuclear Ir^{III} complex dications are reduced in reversible one-electron processes to Ir^{III}_2 complexes of the anion radicals $L^{\bullet -}$. In agreement with the stronger π acceptor character of bptz versus bpip [4,7], the potentials of the bptz complexes (M = Rh and Ir) lie more positively by about 0.5 V, the very similar potentials of rhodium and iridium species support this assignment.

Table 1
Peak and half-wave potentials from cyclic voltammetry [a] of complexes $[Cp^*ClM(\mu\text{-}L)MClCp^*](PF_6)_2$

E [b]	μ-L = bpip		μ-L = bptz	
	M = Ir	(M = Rh)	M = Ir	(M = Rh)
E_1	−0.44	(−0.50)	−0.04	(−0.03)
E_2	−0.83	(−0.76)	−0.97	(−1.06)
E_3	−1.54 [c]	(−1.25)	−1.48	(−1.37)
E_4	−1.54 [c]	(−1.39)	−1.48	(−1.37)
E_5	< −2.7	(−2.45)	−1.93	(−1.44)
E_6			−2.57	(−2.02)
$E_{1'}$	−0.36	(−0.43)	+0.03	(+0.04)
$E_{2'}$	−0.36	(−0.43)	−0.47	(−0.46)
$E_{3'}$	−1.23	(−1.03)	−1.42	(−1.03)
$E_{4'}$	−1.44	(−1.33)	−1.42	(−1.03)
$E_{5'}$	< −2.6	(−2.37)	−1.86	(−1.37)
$E_{6'}$			−2.41	(−1.94)
$E_{1/2}(1)$	−0.40	(−0.47)	0.00	(0.00)
$E_{1/2}(4)$	−1.49	(−1.36)	−1.45	
$E_{1/2}(5)$		(−2.41)	−1.90	(−1.40)

[a] In CH_3CN/0.1 M Bu_4NPF_6 at 100 mV s^{-1} scan rate; potentials versus $FeCp_2^{+/0}$.

[b] For identification of processes see Eqs. (1)–(6) in the text.

[c] Two overlapping one-electron peaks according to spectroelectrochemistry.

Table 2
Absorption maxima [a] of complexes from UV–vis/NIR spectroelectrochemistry [b]

Complex	μ-L = bpip		μ-L = bptz	
	M = Ir	M = Rh	M = Ir	M = Rh
$[(Cp^*ClM)(\mu\text{-L})(MClCp^*)]^{2+}$	320 (11.6)	321 (14)	310 (22.7)	315 (24)
	380sh (7.7)	370 (11)	470sh	358sh
	504 (10.3)	465 (10)	580 (6.6)	536 (5)
	610 (2.9) [c]	–	762 (3.7) [c]	–
$[(Cp^*ClM)(\mu\text{-L})(MClCp^*)]^{\bullet+}$	360 (10.5)	330 (14)	285 (22.0)	289 (24)
	387 (10.7)	402 (14)	428 (4.5)	358sh
	480 (11.6)	451 (13)	490sh	420sh
	533 (8.7)	546 (9)		
	636 (7.6)	690 (4)		
	860 (0.1) [c]			
$[(Cp^*M)(\mu\text{-L})(MClCp^*)]^{+}$	300 (17.2)	321 (21)	277 (17.4)	289 (20)
	382 (16.6)	429 (10)	460sh	470sh
	530 (18.2)	578 (12)	525 (8.4)	
	625 (11.0)	691 (18)	592 (13.7)	641 (15)
$[(Cp^*M)(\mu\text{-L})(MCp^*)]^{+}$	285 [d]	311 (21)	[e]	[e]
	378	452 (7)		
	495sh			
	530	578 (7)		
	680	698 (29)		
	825	877 (9)		
	1070	1142 (0.9)		
	1225	1396 (1.1)		
	1415	1708 (3.2)		
$[(Cp^*M)(\mu\text{-L})(MCp^*)]$	344 (14.7)	298 (19)	310sh (15.0)	289 (21)
	412 (13.1)	383 (13.1)	414 (9.6)	471 (6)
	527 (11.8)	523 (7)	609 (9.7)	527 (7)
			755sh	641sh
	703 (19.5)	698 (33)	820 [b] (11.4)	792 (21)
	926 (0.9)	886 (6)		
	1050 (1.9)	1007 (5)		
	1205 (1.8)	1136 (5)		
$[(Cp^*M)(\mu\text{-L})(MCp^*)]^{\bullet-}$	[f]	[f]	318 (9.7)	294 (11)
			420 (5.7)	466 (11)
			547 (5.8)	543sh
			635 (8.4)	636sh
				792sh
				866 (18)
$[(Cp^*M)(\mu\text{-L})(MCp^*)]^{2-}$	[f]	[f]		348sh
				389sh
				498 (11)
				691 (13)

[a] Absorption maxima λ_{max} in nm (molar extinction coefficients $\varepsilon \times 10^{-3}$ in M^{-1} cm^{-1}).
[b] OTTLE cell; CH_3CN/0.1 M Bu_4NPF_6, except for L = bpip and M = Ir (DMF/0.1 M Bu_4NPF_6).
[c] ^{3}LMCT.
[d] Observed within comproportionation equilibrium.
[e] Not detectable (disproportionation).
[f] Not accessible.

The EPR spectra of the radical complexes show a range of different responses.

The rhodium complexes still show the typical features of systems $(\mu\text{-bptz}^{\bullet-})(ML_n)_2$ [21], i.e. observability at room temperature, small g anisotropy, isotropic g values not far from $g_{electron} = 2.0023$, and, in case of L = bptz, hyperfine coupling from the metal (^{103}Rh, 100% nat. abundance, isotropic hyperfine constant $a_o = 43.85$ mT) and from two non-equivalent pairs of free and metal-coordinated tetrazine nitrogen centers (Fig. 4). The size of the rhodium hyperfine coupling ($a/a_o = 0.012$) and the splitting of the originally equivalent tetrazine N centers suggest a small but non-negligible pertubation of the ligand-based singly occupied MO by metal coordination [21]. No hyperfine resolution is detected for the paramagnetic iridium complexes; an ^{191,193}Ir isotope coupling (^{191}Ir: $I = 3/2$, 37.3% nat. abundance, $a_o = 112.96$ mT; ^{193}Ir: $I = 3/2$, 62.7%, $a_o =$

124.60 mT [22]) could not be observed due to the low nuclear magnetic moment of this isotope and relatively broad lines. Nevertheless, the effect of the 5d metal centers with their large spin-orbit coupling constants [22] are clearly visible through larger g anisotropy g_1-g_3 and stronger deviation of g_{iso} from $g_{electron}$. These effects are most pronounced for [Cp*ClIr(μ-bpip)IrClCp*]$^{\bullet+}$, the EPR signal of which (Fig. 5) is broadened beyond detection at room temperature (Table 3). This situation suggests significant participation of metal orbitals in the singly occupied MO of this particular species; the lower lying π^* orbital of bptz causes the corresponding complex to exhibit less metal contribution.

UV–vis spectroelectrochemistry (Fig. 2, Table 2) is in agreement with the interpretation of a ligand-centered first reduction; the bptz anion radical does not exhibit major detectable $\pi-\pi^*$ bands in the visible region and the weak $n-\pi^*$ band experiences only a small shift. A ligand-to-metal charge transfer (LMCT) transition from electron-rich bptz$^{\bullet-}$ to Ir(III) is not detected as a major feature. The compounds [Cp*ClM(μ-bpip)MClCp*]$^{\bullet+}$ have several absorptions in the visible region similarly as the free anion radical bpip$^{\bullet-}$ [9].

This ligand-centered one-electron reduction of the dinuclear complexes stands in contrast to mononuclear complexes [Cp*ClIr(α-diimine)]$^+$ which exhibit a Cl^--dissociative metal-based two-electron process as first reduction feature [13,14,23].

$$[Cp^*ClIr(\mu\text{-}L)IrClCp^*]^{2+} + e^- \underset{E_{1'}}{\overset{E_1}{\rightleftharpoons}} [Cp^*ClIr(\mu\text{-}L)IrClCp^*]^{\bullet+} \quad (1)$$

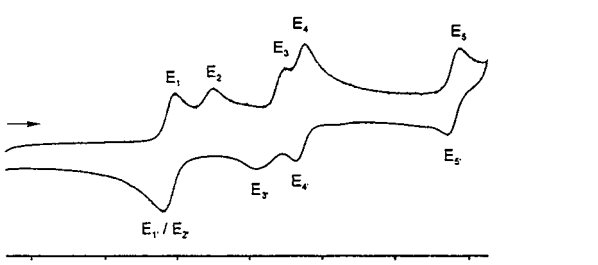

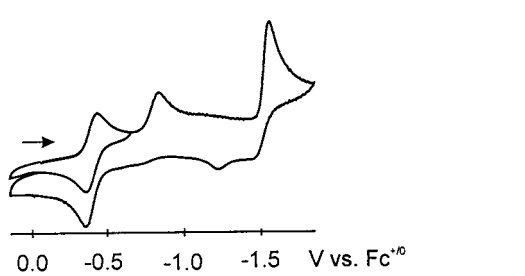

Fig. 1. Cyclic voltammograms of [Cp*ClRh(μ-bpip)RhClCp*](PF$_6$)$_2$ (top) and [Cp*ClIr(μ-bpip)IrClCp*](PF$_6$)$_2$ (bottom) in CH$_3$CN/0.1 M Bu$_4$NPF$_6$ at 100 mV s^{-1} scan rate.

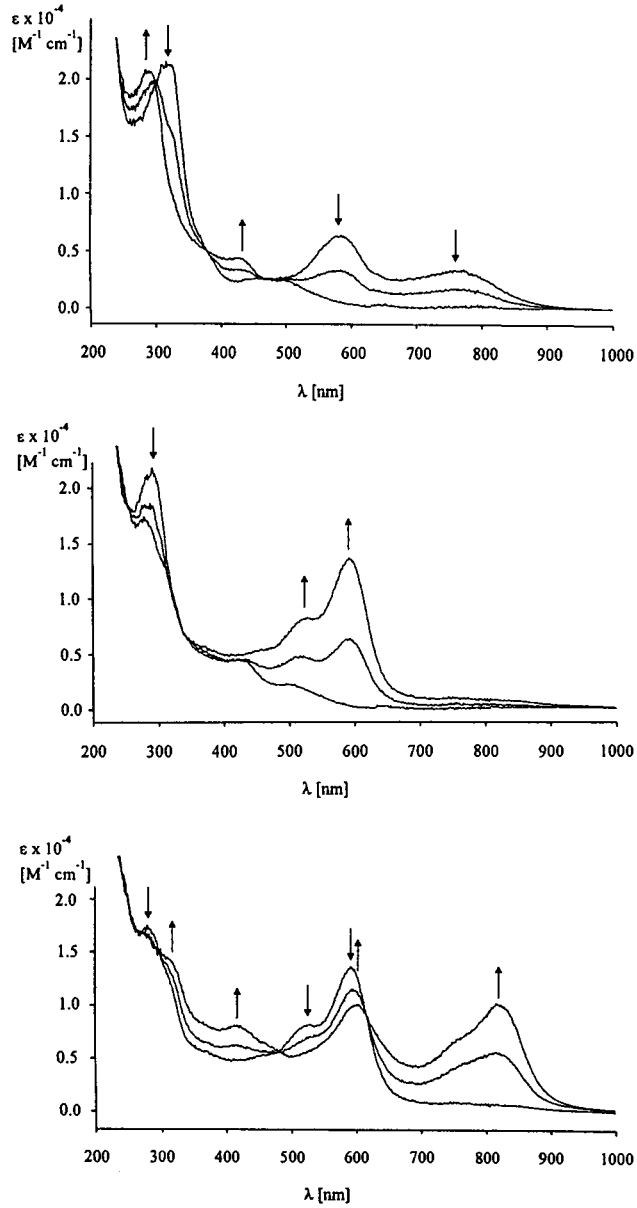

Fig. 2. Spectroelectrochemistry of the transitions [Cp*ClIr(μ-bptz)IrClCp*]$^{2+\rightarrow+}$ (top), [Cp*ClIr(μ-bptz)IrClCp*]$^+ \rightarrow$[Cp*Ir(μ-bptz)IrClCp*]$^+$ (center) and [Cp*Ir(μ-bptz)IrClCp*]$^+ \rightarrow$[Cp*Ir(μ-bptz)IrCp*] (bottom) in CH$_3$CN/0.1 M Bu$_4$NPF$_6$.

The first chloride dissociation occurs only in the second step as a one-electron EC process with the typical shift [12,13] of cathodic and anodic peak potentials $E_2-E_{2'}$ of about 0.5 V. This indicates that there is only one of the two equivalent metal centers affected.

$$[Cp^*ClIr(\mu\text{-}L)IrClCp^*]^{\bullet+} + e^- \overset{E_2}{\rightarrow} [Cp^*Ir(\mu\text{-}L)IrClCp^*]^+ + Cl^- \quad (2)$$

$$[Cp^*Ir(\mu\text{-}L)IrClCp^*]^+ - e^- \overset{E_{2'}}{\rightarrow} [Cp^*Ir(\mu\text{-}L)IrClCp^*]^{2+} \quad (2')$$

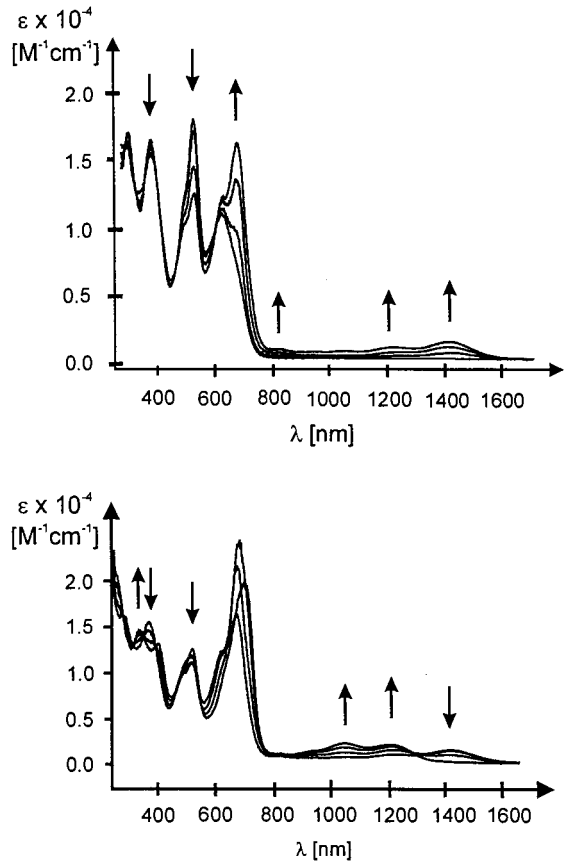

Fig. 3. Spectroelectrochemistry of the transitions $[Cp^*Ir(\mu\text{-bpip})IrClCp^*]^{+} \rightarrow [Cp^*Ir(\mu\text{-bpip})IrCp^*]^{+}$ (top) and $[Cp^*Ir(\mu\text{-bpip})IrCp^*]^{+ \rightarrow 0}$ (bottom) in DMF/0.1 M Bu_4NPF_6.

There is much less difference between the bptz and bpip complexes for E_2 and $E_{2'}$ (Table 1), confirming the metal-based character of this process.

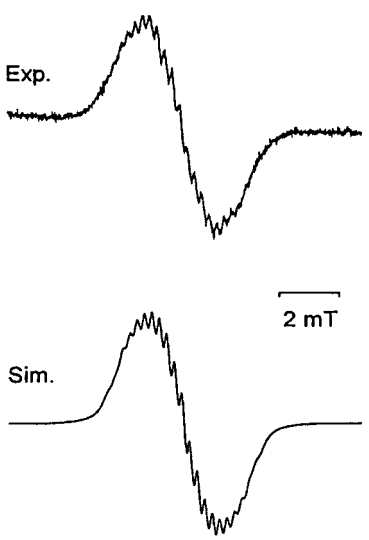

Fig. 4. EPR spectrum of electrogenerated $[Cp^*ClRh(\mu\text{-bptz})RhClCp^*]^{\bullet +}$ in CH_3CN/0.1 M Bu_4NPF_6 at 293 K (top); computer simulation with the data from Table 3 and 0.32 mT linewidth.

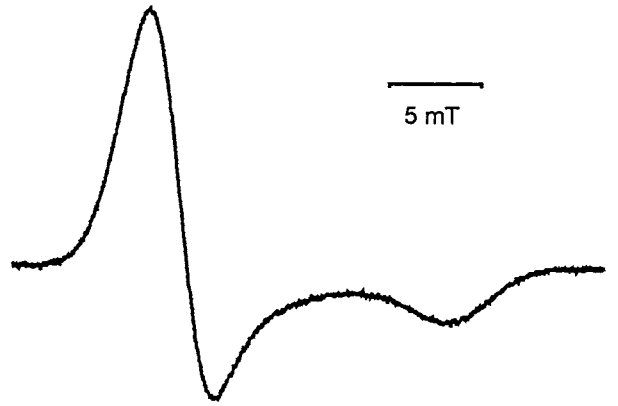

Fig. 5. EPR spectrum of electrogenerated $[Cp^*ClIr(\mu\text{-bpip})IrClCp^*]^{\bullet +}$ in CH_3CN/0.1 M Bu_4NPF_6 at 110 K.

Spectroelectrochemically, the reduction and chloride dissociation are accompanied by the appearance of an intense charge transfer band in the visible which, to a first approximation [12,13,23], can be interpreted as a $d(Ir^{I}) \rightarrow \pi^*(\mu\text{-L})$ metal-to-ligand charge transfer (MLCT). It should be noted here that reaction (2) implies an intramolecular electron transfer from the ligand to the metal so that one bound anion radical ligand and one external electron combine to effect the chloride-dissociative $Ir^{III} \rightarrow Ir^{I}$ transition. The conjugated bridging ligand thus acts as an electron reservoir [5] to pick up and store one charge equivalent before the necessary number of two electrons for the producing step is collected.

The following electrode processes differ for the bpip and bptz systems: for the bptz compounds, there are two close lying waves of which the first involves two electrons ($E_{3,4}$), leading to a neutral dinuclear complex, followed by a one-electron step (E_5, $E_{5'}$).

$$[Cp^*Ir(\mu\text{-bptz})IrClCp^*]^{+} + 2e^{-} \underset{E_{3'}=E_{4'}}{\overset{E_3=E_4}{\rightleftharpoons}} Cp^*ClIr(\mu\text{-bptz})IrCp^* + Cl^{-} \qquad (3+4)$$

This interpretation is supported by spectroelectrochemistry which reveals a long-wavelength shift of the

Table 3
EPR data of complexes $[Cp^*ClM(\mu\text{-L})MClCp^*]^{\bullet +}$ [a]

M	μ-L	g_1, g_2, g_3 (110 K)	g_{iso}
Ir	bpip	1.994, 1.994, 1.9156	1.968 [b]
Ir	bptz	2.019, 1.991, 1.962	1.9917 (293 K)
Rh	bpip	[c]	1.9934 (270 K)
Rh	bptz	2.002, 2.002, 1.9914	1.9990 [d] (293 K)

[a] Obtained through electrolytic reduction of dicationic precursors in CH_3CN/0.1 M Bu_4NPF_6.

[b] Calculated from g_1–g_3, spectrum detectable only below 200 K.

[c] Small g component splitting.

[d] Hyperfine structure: $a(^{14}N) = 0.24$ and 0.74 mT, $a(^{103}Rh) = 0.53$ mT.

charge transfer band (Fig. 2) as is well known for mono- and dinuclear complexes of π acceptor ligands with electron-rich metals [4,6].

For the bpip complexes, the loss of the second chloride occurs in a more complicated way, this ECE process being split into an EC step ($E_{3'}$ + Cl dissociation) and an E process (E_4). For the rhodium system, the two features are clearly distinguishable in the cyclic voltammogram (Fig. 1), revealing a potential range of about 140 mV for the Rh^{II}/Rh^{I} mixed-valent intermediate ($K_c = 10^{2.4}$). Spectroelectrochemically, this unusual state is distinguished by long-wavelength intervalence charge transfer (IVCT) bands in the near infrared region ($\lambda > 1200$ nm) [8]; similar features were noted for the Creutz–Taube ion ($\lambda_{IVCT} = 1570$ nm) [2].

The diiridium analogue does not exhibit a clear splitting $E_3C + E_4$ in the cathodic scan of the cyclic voltammogram at 100 V s^{-1} (Fig. 1); however, the corresponding two-electron feature is complemented by two different anodic peak potentials $E_{3'}$ and $E_{4'}$ (Table 1). Careful spectroelectrochemistry (Fig. 3) reveals that there is a comproportionation equilibrium in which the Ir^{II}/Ir^{I} intermediate [Cp*Ir(μ-bpip)IrCp*]$^+$ is apparent from NIR absorption features (Table 2). The slightly higher energies of these IVCT bands in the Ir versus Rh case suggest stronger metal–ligand–metal interaction (Table 2). The loss of the second chloride is much slower for the iridium complex which results in a smaller shift of E_3 to positive potentials and an apparently two-electron cathodic signal at conventional scan rates.

$$[Cp^*Ir(\mu\text{-bpip})IrClCp^*]^+ + e^- \overset{E_3}{\rightarrow} [Cp^*Ir(\mu\text{-bpip})IrClCp^*]^+ + Cl^- \quad (3)$$

$$[Cp^*Ir(\mu\text{-bpip})IrCp^*]^+ - e^- \overset{E_{3'}}{\rightarrow} [Cp^*Ir(\mu\text{-bpip})IrCp^*]^{2+} \quad (3')$$

$$[Cp^*Ir(\mu\text{-bpip})IrCp^*]^+ + e^- \underset{E_{4'}}{\overset{E_4}{\rightleftharpoons}} Cp^*Ir(\mu\text{-bpip})IrCp^* \quad (4)$$

The coupling of d^7/d^8 metal centers through a π acceptor bridge is unusual because Pt^{III}/Pt^{II} species were shown to exhibit very little such interaction [6,24]. The reason for the failure to observe such interaction for platinum species and for the bptz-bridged systems presented here lies in the incompatibility between d_σ metal orbitals and ligand π^* MOs [6,24]; the sterically encumbered situation through methyl and phenyl substituents for the dinuclear bpip complexes probably allows for a limited such interaction through σ/π orbital mixing.

The neutral bpip- and bptz-bridged compounds exhibit long-wavelength CT bands (Figs. 2 and 3) from transitions between orbitals of metal/ligand mixed character; these bands lie in the near infrared (850–1250 nm) but not as low in energy as the IVCT bands of the bpip compounds (1000–1800 nm). For L = bpip, both sets of transitions exhibit a typical three-band pattern with differences between 1100 and 1600 cm^{-1} (vibrational structuring) ([9]c, [20,23,25]).

Concerning the potentials, the small difference between bptz and bpip species again confirms the largely metal-based processes (3), (3′) and (4). The potentials of the iridium analogues lie at more negative potentials in agreement with the very strongly π electron donating character of Cp*Ir [13,26]. An interesting value in terms of coupling between the two reaction centers is the difference $E_3 - E_2$ which varies from 310 mV (L = bptz, M = Rh) to 710 mV for L = bpip, M = Ir. In view of the approximately constant metal–metal distances this number reflects stronger interaction for the iridium case and for the bpip-bridged systems.

One-electron reduction of the neutral compounds leads to monoanionic species which could be studied for L = bptz.

$$Cp^*M(\mu\text{-bptz})MCp^* + e^- \underset{E_{5'}}{\overset{E_5}{\rightleftharpoons}} [Cp^*M(\mu\text{-bptz})MCp^*]^- \quad (5)$$

Intense charge transfer bands in the visible region and the EPR result for the rhodium system, i.e. large g anisotropy ($g_1 = 2.151$, $g_2 = 2.035$, $g_3 = 1.960$), the absence of ligand hyperfine splitting and the broadening of lines at higher temperatures [8] suggest strong orbital mixing between the metals and the bridging ligand [16,23,26]. Strong metal/ligand interaction is also evident from the very different potentials E_5 which are much more negative for the bpip system (ligand effect) and for the iridium analogues (metal influence).

The last recorded reduction is a quasi-reversible one-electron process which leads to a dianion in which both metal centers and the bptz ligand exist in their reduced states. The absorption in the long-wavelength region is due to a $\pi \rightarrow \pi^*$ intra-ligand transition of $bptz^{2-}$.

$$[Cp^*M(\mu\text{-bptz})MCp^*]^- + e^- \underset{E_{6'}}{\overset{E_6}{\rightleftharpoons}} [Cp^*M(\mu\text{-bptz})MCp^*]^{2-} \quad (6)$$

Wider variations of ligands will have to clarify the origins and extent of metal-metal interaction, the reasons for decoupling of ECE processes, and the electron reservoir function of the ligands in the eventual quest for constructing multielectron redox systems and catalysts.

3. Experimental

Instrumentation and spectroelectrochemical techniques were described previously [13b] as were the compounds [Cp*ClRh(μ-L)RhClCp*]$(PF_6)_2$ [8].

Compounds [Cp*ClIr(μ-L)IrClCp*]$(PF_6)_2$ were obtained from reacting $[Cp^*Cl_2Ir]_2$ [19] with two equivalents of $AgPF_6$ in acetone and addition of one equivalent of the bridging ligand L [4,7] to the filtrate after removal of AgCl through celite. After 1 h the deeply colored solutions were reduced in volume, filtered, and the filtrate treated with excess Bu_4NPF_6 to yield the purplish–black (bpip) or blue–black (bptz) products in about 80% yield.

[Cp*ClIr(μ-bpip)IrClCp*]$(PF_6)_2$. Anal. calc. for $C_{40}H_{48}Cl_2F_{12}Ir_2N_4P_2$ (1330.13): C, 36.12; H, 3.64; N, 4.21%. Found: C, 36.17; H, 3.67; N, 4.09%. ^{1}H-NMR (CD_3NO_2; *cis* and *trans* isomers A and B in a 1:3 ratio): $\delta = 1.63$(B) and 1.66(A) (s, 30 H, Cp*), 3.02(A) and 3.04(B) (s, 6H, CH_3), 7.69(A,B) (m, 6H, H^{Ph}), 7.83(A,B) (m, 4H, H^{Ph}), 9.60(B) and 9.63(A) (s, 2H, H^{Pz}).

[Cp*ClIr(μ-bptz)IrClCp*]$(PF_6)_2$. Anal. calc. for $C_{32}H_{38}Cl_2F_{12}Ir_2N_6P_2$ (1251.81): C, 30.70; H, 3.06; N, 6.71%. Found: C, 30.96; H, 3.53; N, 6.13%. ^{1}H-NMR (CD_3NO_2): $\delta = 2.00$ (s, 30 H, Cp*), 8.35 (ddd, 2H, $H^{5,5'}$), 8.68 (dt, 2H, $H^{4,4'}$), 9.21 (d, 2H, $H^{6,6'}$), 9.24 (d, 2H, $H^{3,3'}$). $^3J(H^3H^4) = 7.9$ Hz, $^3J(H^4H^5) = 6.7$ Hz, $^3J(H^5H^6 = 5.5$ Hz.

Acknowledgements

This work was supported by Deutsche Forschungsgemeinschaft (DFG, SFB 270). We thank Degussa AG for a loan of $IrCl_3$.

References

[1] (a) J.R. Bolton, N. Mataga, G. McLendon (Eds.), Electron Transfer in Inorganic, Organic and Biological Systems, Adv. Chem. Ser. No. 228, ACS, Washington, DC, 1991. (b) H. Taube, Angew. Chem. 96 (1984) 315. Angew. Chem. Int. Ed. Engl. 23 (1984) 329.
[2] C. Creutz, Prog. Inorg. Chem. 30 (1983) 1.
[3] J. Poppe, M. Moscherosch, W. Kaim, Inorg. Chem. 32 (1993) 2640.
[4] W. Kaim, S. Kohlmann, Inorg. Chem. 26 (1987) 68.
[5] D. Astruc, Electron Transfer and Radical Processes in Transition Metal Chemistry, VCH, Weinheim, 1995.
[6] A. Klein, S. Hasenzahl, W. Kaim, J. Fiedler, Organometallics 17 (1998) 3532.
[7] (a) A. Klein, V. Kasack, R. Reinhardt, T. Sixt, T. Scheiring, S. Zalis, J. Fiedler, W. Kaim, J. Chem. Soc. Dalton Trans., submitted for publication. (b) W. Kaim, S. Ernst, V. Kasack, J. Am. Chem. Soc. 112 (1990) 173.
[8] W. Kaim, R. Reinhardt, J. Fiedler, Angew. Chem. 109 (1997) 2600. Angew. Chem. Int. Ed. Engl. 36 (1997) 2493.
[9] (a) H. Brunner, W.A. Herrmann, Chem. Ber. 105 (1972) 770. (b) L.H. Polm, C.J. Elsevier, G. van Koten, J.M. Ernsting, D.J. Stufkens, K. Vrieze, R.R. Andrea, C.H. Stam, Organometallics 6 (1987) 1096. (c) R.W. Balk, D.J. Stufkens, A. Oskam, Inorg. Chim. Acta 34 (1979) 267. (d) H.A. Nieuwenhuis, A. van Loon, M.A. Moraal, D.J. Stufkens, A. Oskam, K. Goubitz, Inorg. Chim. Acta 232 (1995) 19.
[10] T. Stahl, V. Kasack, W. Kaim, J. Chem. Soc. Perkin Trans. 2 (1995) 2127.
[11] (a) U. Kölle, M. Grätzel, Angew. Chem. 99 (1987) 572. Angew. Chem. Int. Ed. Engl. 26 (1987) 568. (b) U. Kölle, B.-S. Kang, P. Infelta, P. Compte, M. Grätzel, Chem. Ber. 122 (1989) 1869.
[12] M. Ladwig, W. Kaim, J. Organomet. Chem. 419 (1991) 233.
[13] (a) M. Ladwig, W. Kaim, J. Organomet. Chem. 439 (1992) 79. (b) W. Kaim, R. Reinhardt, E. Waldhör, J. Fiedler, J. Organomet. Chem. 524 (1996) 195.
[14] (a) C. Cosnier, A. Deronzier, N. Vlachopoulos, J. Chem. Soc. Chem. Commun. (1989) 1259. (b) S. Chardon-Noblat, S. Cosnier, A. Deronzier, N. Vlachopoulos, J. Electroanal. Chem. 352 (1993) 213. (c) R. Ziessel, Angew. Chem. 103 (1991) 863. Angew. Chem. Int. Ed. Engl. 30 (1991) 844. (d) R. Ziessel, J. Chem. Soc. Chem. Commun. (1988) 16. (e) R. Ziessel, J. Am. Chem. Soc. 115 (1993) 118. (f) M.-T. Youinou, R. Ziessel, J. Organomet. Chem. 363 (1989) 1987. (g) C. Caix, S. Chardon-Noblat, A. Deronzier, R. Ziessel, J. Electroanal. Chem. 362 (1993) 301. (h) A. Deronzier, J.-C. Moutet, Platinum Met. Rev. 42 (1998) 60.
[15] R. Reinhardt, W. Kaim, Z. Anorg. Allg. Chem. 619 (1993) 1998.
[16] S. Greulich, W. Kaim, A. Stange, H. Stoll, J. Fiedler, S. Zalis, Inorg. Chem. 35 (1996) 3998.
[17] R. Reinhardt, S. Greulich, F. Baumann, J. Fiedler, W. Kaim in: F. Philipps (Ed.), Wasserstoff als Energieträger, Universität Stuttgart, 1997, p 125. ISBN 3-00-001796-8.
[18] (a) R. Ruppert, S. Herrmann, E. Steckhan, J. Chem. Soc. Chem. Commun. (1988) 1150. (b) E. Steckhan, S. Herrmann, R. Ruppert, E. Dietz, M. Frede, E Spika, Organometallics, 10 (1991) 1568. (c) D. Westerhausen, S. Herrmann, W. Hummel, E. Steckhan, Angew. Chem. 104 (1992) 1496. Angew. Chem. Int. Ed. Engl. 31 (1992) 1529. (d) E. Steckhan, S. Herrmann, R. Ruppert, J. Thömmes, C. Wandrey, Angew. Chem. 102 (1990) 445. Angew. Chem. Int. Ed. Engl. 29 (1990) 388.
[19] C. White, A. Yates, P.M. Maitlis, Inorg. Synth. 29 (1992) 228.
[20] F. Baumann, A. Stange, W. Kaim, Inorg. Chem. Commun. 1 (1998) 305.
[21] (a) W. Kaim, S. Kohlmann, Inorg. Chem. 25 (1986) 3442. (b) S. Kohlmann, V. Kasack, E. Roth, W. Kaim, J. Chem. Soc. Faraday Trans. 1, 85 (1989) 4047.
[22] J.A. Weil, J.R. Bolton, J.E. Wertz, Electron Paramagnetic Resonance, Wiley, New York, 1994.
[23] W. Kaim, R. Reinhardt, M. Sieger, Inorg. Chem. 33 (1994) 4453.
[24] A. Klein, W. Kaim, J. Fiedler, S. Zalis, Inorg. Chim. Acta 264 (1997) 269.
[25] W. Kaim, S. Kohlmann, A.J. Lees, T.L. Snoeck, D.J. Stufkens, M.M. Zulu, Inorg. Chim. Acta 210 (1993) 159.
[26] W. Bruns, W. Kaim, M. Ladwig, B. Olbrich-Deussner, T. Roth, B. Schwederski, in: A.J.L. Pombeiro, J. McCleverty (Eds.), Molecular Electrochemistry of Inorganic, Bioinorganic, Organometallic Compounds, Kluwer, Dordrecht, 1993, p. 255.